

## Development and operation of a high-throughput accurate-wavelength lens-based spectrometers)

Ronald E. Bell

Citation: [Review of Scientific Instruments](#) **85**, 11E404 (2014); doi: 10.1063/1.4884612

View online: <http://dx.doi.org/10.1063/1.4884612>

View Table of Contents: <http://scitation.aip.org/content/aip/journal/rsi/85/11?ver=pdfcov>

Published by the [AIP Publishing](#)

---

### Articles you may be interested in

[High accuracy wavelength calibration for a scanning visible spectrometers\)](#)

Rev. Sci. Instrum. **81**, 10D732 (2010); 10.1063/1.3489975

[High-throughput accurate-wavelength lens-based visible spectrometers\)](#)

Rev. Sci. Instrum. **81**, 10D731 (2010); 10.1063/1.3485096

[A high-precision five-degree-of-freedom measurement system based on laser collimator and interferometry techniques](#)

Rev. Sci. Instrum. **78**, 095105 (2007); 10.1063/1.2786272

[Design and implementation of a high-resolution, high-efficiency optical spectrometer](#)

Rev. Sci. Instrum. **73**, 3737 (2002); 10.1063/1.1510574

[Compact fiber-optic fluorosensor using a continuous-wave violet diode laser and an integrated spectrometer](#)

Rev. Sci. Instrum. **71**, 3004 (2000); 10.1063/1.1305814

---



# Development and operation of a high-throughput accurate-wavelength lens-based spectrometer<sup>a)</sup>

Ronald E. Bell<sup>b)</sup>

*Princeton Plasma Physics Laboratory, Princeton, New Jersey 08543, USA*

(Presented 4 June 2014; received 1 June 2014; accepted 4 June 2014; published online 11 July 2014)

A high-throughput spectrometer for the 400–820 nm wavelength range has been developed for charge exchange recombination spectroscopy or general spectroscopy. A large 2160 mm<sup>-1</sup> grating is matched with fast  $f/1.8$  200 mm lenses, which provide stigmatic imaging. A precision optical encoder measures the grating angle with an accuracy  $\leq 0.075$  arc sec. A high quantum efficiency low-etaloning CCD detector allows operation at longer wavelengths. A patch panel allows input fibers to interface with interchangeable fiber holders that attach to a kinematic mount at the entrance slit. Computer-controlled hardware allows automated control of wavelength, timing, f-number, automated data collection, and wavelength calibration. © 2014 AIP Publishing LLC. [<http://dx.doi.org/10.1063/1.4884612>]

## I. INTRODUCTION

A scanning visible spectrometer has been designed to complement and expand the capabilities of the existing charge exchange recombination spectroscopy (CXRS) diagnostics suite<sup>1</sup> on the National Spherical Torus Experiment-Upgrade (NSTX-U) and to serve as a general plasma spectroscopy tool. The existing spectrometers are fixed-wavelength transmission grating spectrometers featuring high throughput ( $f/1.8$ ) optics, stigmatic imaging, and wavelength stability.<sup>2</sup> Adding a scanning capability across the visible and into the near infrared, while retaining the best features of the transmission grating spectrometers would extend the capability and flexibility of the CXRS diagnostic suite and provide a flexible tool for more general plasma spectroscopy.

This operating spectrometer is an extension of a prototype spectrometer<sup>3</sup> that demonstrated the utility of the precision encoder to calibrate the wavelength to high accuracy, by fitting all relevant spectrometer parameters using emission lines that span the spectral range of the spectrometer.<sup>4</sup> The goal was to calibrate the absolute wavelength to within the uncertainty in the toroidal velocity measurement under good conditions ( $\sim 0.3$  km/s). Typical commercial spectrometers can determine the absolute wavelength to  $\sim 0.1$  nm after the grating has been moved. With a precision encoder developed by NASA<sup>5</sup> to measure the grating angle, the absolute wavelength can be determined to  $\sim 0.001$  nm. At this wavelength accuracy, variations in the index of refraction due to changes in air temperature and pressure can be significant. Likewise, small temperature changes causing thermal expansion of the grating can change the effective groove spacing. Environmental monitors of temperature and pressure are incorporated into the wavelength calibration to maintain accuracy.

Like the prototype spectrometer,<sup>3</sup> the new spectrometer uses a large reflection grating, fast commercial telephoto lenses ( $f/1.8$ ), and a precision encoder to measure the grating angle. Additional features include a high quantum-efficiency (QE) charge coupled device (CCD) for the detector, a fiber optic patch panel for flexibility of input plasma sources, and multiple interchangeable fiber holders for quick exchanges of input fibers. For the last year, the new spectrometer has been operating on the Lithium Tokamak Experiment<sup>6</sup> (LTX) to support LTX plasma spectroscopy, to test the spectrometer hardware, and to develop and refine the automated software control for data acquisition and calibrations.

## II. SPECTROMETER

The spectrometer is laid out on a 2 × 4 ft optical table (see Fig. 1). The wavelength range of the spectrometer is 400–820 nm. The lower end of this range is determined by the transmission of the glass optics in the lenses. The upper end is near the limit of the grating angle. A small angle between the collimating and focusing lenses ( $\sim 20^\circ$ ) allows the wavelength to extend into the near infrared while requiring a larger footprint for the spectrometer. The reciprocal linear dispersion varies from about 2.3 nm/mm at 400 nm to 1.4 nm/mm at 820 nm.

Optical fibers of varying sizes are used on NSTX-U. A patch panel on the spectrometer accepts 47 Sub Multi Assembly (SMA) terminated fibers of three sizes (210, 400, and 600  $\mu\text{m}$  core). Short lengths of like-sized SMA terminated fibers connect the patch panel to custom fiber holders that are mounted at the manually adjustable entrance slit. The number of fibers in each holder depends on fiber size; there are 23 fibers with a 210  $\mu\text{m}$  core, 13 fibers with a 400  $\mu\text{m}$  core, and 9 fibers with a 600  $\mu\text{m}$  core. The fiber holders are designed to be interchangeable. Each fiber holder is made up of a barrel into which the fibers are potted that mounts inside a sleeve allowing the fibers to be rotated about and translated along the optical axis, so that each fiber holder is precisely aligned with the entrance slit. The assembly of barrel and

<sup>a)</sup>Contributed paper, published as part of the Proceedings of the 20th Topical Conference on High-Temperature Plasma Diagnostics, Atlanta, Georgia, USA, June 2014.

<sup>b)</sup>Author to whom correspondence should be addressed. Electronic mail: [rbell@pppl.gov](mailto:rbell@pppl.gov)

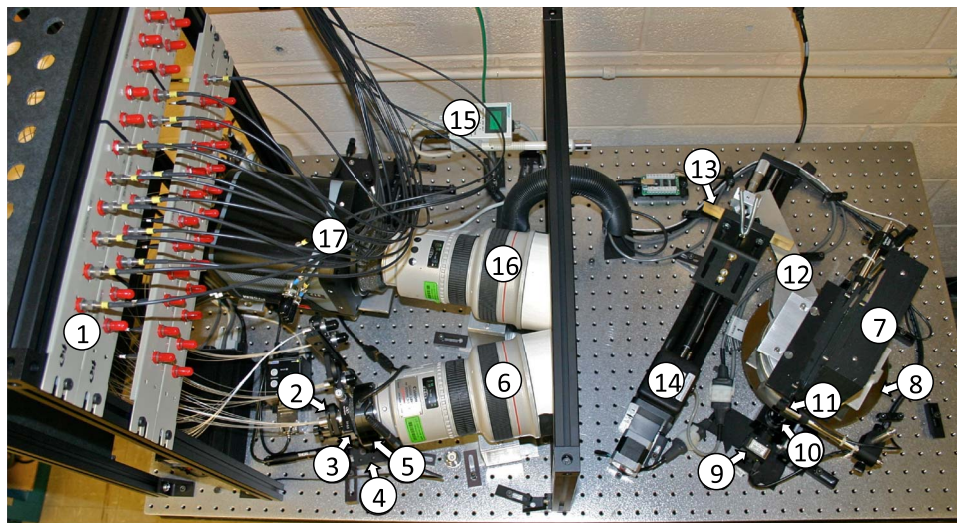


FIG. 1. Overview of the spectrometer. Components include (1) fiber optic patch panel, (2) fiber holder, (3) entrance slit, (4) translation stage for slit assembly, (5) lens controller, (6) collimating lens, (7) grating, (8) encoder disk, (9) encoder camera, (10) microscope objective and 45° mirror, (11) LED, (12) tangent arm, (13) pusher plate, (14) stepping motor and slide, (15) thermometer and barometer, (16) focusing lens, and (17) CCD camera.

sleeve is mounted into a carriage, originally intended for one-inch optics that magnetically couples to a back plate. The back plate is attached to the entrance slit assembly. Intended for precise alignment of one-inch optics, the commercially available kinematic mounts allow easy swapping of fibers when desired. An extra fiber holder serves as a calibration tool with 13 unterminated fibers that can be illuminated with a calibration lamp.

Two telephoto lenses, Canon 200 mm  $f/1.8$  EF, are used for collimating and focusing optics. Collection optics on NSTX-U are  $f/1.8$ - $f/2$ , so the input fibers are well matched to the input optics. An electronic lens controller is attached to the collimating lens, so that the lens aperture can be computer controlled, extending the dynamic range of the optically fast spectrometer when encountering bright emission lines. The clear aperture of the lens is 110 mm. A shift of the focus of the lens as a function of wavelength due to chromatic aberration is observed as a change in apparent line width.<sup>3</sup> This aberration can be corrected with a small shift ( $<0.5$  mm) of the entrance slit assembly along the optical axis as the wavelength is changed. A stepping-motor controlled translation stage makes this adjustment.

A large ruled grating, 154 mm wide and 128 mm high with a spatial frequency of  $2160 \text{ mm}^{-1}$  and a blaze of 500 nm, match the full aperture of the lenses. This grating is about 50% efficient for unpolarized light. The computed effective  $f/\#$  increases at wavelengths above 600 nm ( $f/2$  at 700 nm and  $f/2.5$  at 820 nm), due to the oblique angle of the rotated grating at longer wavelengths.

The grating is aligned with respect to a grating holder that is positioned atop a precision rotary stage. A 100 mm radius encoder disk and a 25.4 cm tangent arm are affixed to the rotary stage. The grating, encoder, and tangent arm turn as a unit. A steel ball at the end of the tangent arm is held onto a pusher plate, which is mounted on a stepping-motor controlled slide. The slide advances  $1.58 \mu$  per step, 400 steps per revolution with a total possible travel range of 31.7 cm. The slide is positioned such that the grating can be rotated from

zero order up to 820 nm. The ability to position the grating at zero orders aids alignment and calibration.

The encoder disk has an outer ring with a pattern consisting of a  $4 \times 4$  array of code bits that indicate the local angle. There are 10 800 code groups around the disk, every 2 arc min. With each code group is a long fiducial marker whose precise centroid can be determined with high accuracy. The encoder pattern is illuminated with a light-emitting diode (LED) while a small USB operated complementary metal-oxide semiconductor (CMOS) camera ( $752 \times 480$ ,  $6 \mu\text{m}$  pixels) behind a microscope objective captures the image of about code groups and fiducial markers. Software analyzes the images to produce the local encoder angle. Radial runout of the rotary stage ( $<0.51 \mu\text{m}$ ) or nonconcentric alignment of the encoder disk with respect to the axis would be interpreted by a single encoder camera as rotation. Using two encoder cameras located precisely  $180^\circ$  apart cancels the error due to runout or misalignment of the disk. The overall accuracy of the angular measurement is better than 0.075 arc sec, which corresponds to  $\sim 0.0005$  nm (equivalent to  $\sim 0.3$  km/s velocity, if measuring a wavelength shift). Measuring the actual grating angle is precise, and independent of the thermal expansion in the sine drive or backlash of the leadscrew.

The detector for the spectrometer has  $512 \times 512$   $16 \mu\text{m}$  pixels (Princeton Instruments ProEm camera with back-illuminated eXelon CCD). This detector has a 64-bit dynamic range and features high QE ( $\sim 95\%$  at 650 nm) and is designed to eliminate issues with an etalon-like interference pattern often observed in thinned back-illuminated CCDs due to the silicon becoming more transparent at longer wavelengths (above  $\sim 700$  nm). A programmable function generator is used to provide timing signals for each frame of data taken with the detector. A six-axis mount for the camera allows precise alignment of the CCD with the image plane.

Changes in air temperature and pressure are measured with a computer-controlled thermometer ( $\pm 0.1^\circ\text{C}$ ) and barometer ( $\pm 2$  hPa) to allow computation of the index of



FIG. 2. Spectrometer, computer, and all associated hardware are shown on mobile cart at LTX facility.

refraction. Changes in refractive index due to the relative humidity are small with respect to the intended wavelength accuracy and are neglected. The bulk temperature of the grating is measured with a thermistor mounted on the back of the grating ( $\pm 0.015^\circ\text{C}$ ) to compute thermal expansion of the BK7 grating blank.

A light-tight enclosure encases the grating assembly and sine drive. A mobile cart holds the optical table, computer, and all supporting devices (see Fig. 2). Setting up the spectrometer after it has been moved into place involves connecting an AC power cord, an Ethernet cable, a trigger for the function generator, and input fibers to the patch panel.

### III. AUTOMATION

A Windows based computer running Visual Basic is used to control all of the devices on the spectrometer. The interactive data language (IDL), which can be called by Visual Basic, is used for higher level computations, e.g., line fitting. MDSplus is used for storing the spectrometer parameters and the data from the detector's camera. Win-spec software is called by Visual Basic to control the CCD camera's function.

A detailed Visual Basic user interface controls all relevant functions of each of the devices on the spectrometer, including the stepping motors for the sine drive and the slit translation, the CMOS cameras for the encoder, the illumination LEDs, the aperture of the input lens, the thermometer/barometer and the thermistor/thermometer for grating temperature, the function generator for camera timing, and the CCD camera. The interface to the devices includes four USB ports, four Serial ports, and two Ethernet ports. Complex sequences are programmed to support automated data acquisition or automatic calibrations.

Calibrations relate central wavelength to the appropriate stepping motor position and the entrance slit position to the appropriate wavelength.

For data acquisition, MDS events are used to signal to the spectrometer that a discharge sequence has been started. Upon receiving the event, which contains the discharge number, the LEDs and encoder cameras are activated and scanned, the grating angle is measured, the environmental measurements are polled, and all spectrometer data are written to the MDSplus database. The CCD camera is readied to await the trigger for the function generator. After the CCD camera is triggered all data are automatically written to the MDSplus database.

For wavelength calibration, emission lines from a mercury calibration lamp are used. After the calibration fibers are installed and the calibration lamp turned on a press of a button launches the wavelength calibration. Given a list of wavelengths, the automated task will move the spectrometer to a wavelength, adjust the exposure time or lens aperture as needed, determine the nominal dispersion, move the emission line to multiple positions on the detector while recording the images and storing the relevant spectrometer parameters. These steps are repeated for all wavelengths, the line positions are fitted for all vertical positions, and a fit to the relevant spectrometer parameters is performed. For seven emission lines at 5 locations each takes approximately 16 min, including the exposure times and translation of the sine drive.

Some tasks must be done manually, e.g., exchanging fiber holders or turning on a calibration lamp. The entrance slit is also manually adjusted, though an automatic sequence to continuously measure the instrumental width (at zero order) improves the accuracy of the set slit width.

### IV. OPERATION

With NSTX-U now in a construction phase, the spectrometer is being tested at LTX while supporting the plasma spectroscopy effort there. A toroidal array of 13 existing fiber optics was installed on the spectrometer. Frame times of 2.5 ms are used for the  $\sim 40$  ms plasma discharges. Emission lines of Li I-III, C I-IV, and O I-II are measured. Line fitting and analysis routines for evaluating spectral data are ongoing.

Priority was given to automating the data acquisition, which is now routine. Automated wavelength calibrations are just beginning. The development of the software and techniques for evaluating the spectrometer remain under development.

### ACKNOWLEDGMENTS

The author would like to acknowledge the support of B. C. Stratton. This work was supported by the U. S. Department of Energy under Contract No. DE-AC02-09CH11466.

<sup>1</sup>R. E. Bell and R. Feder, *Rev. Sci. Instrum.* **81**, 10D724 (2010).

<sup>2</sup>R. E. Bell, *Rev. Sci. Instrum.* **75**, 4158 (2004)

<sup>3</sup>R. E. Bell and F. Scotti, *Rev. Sci. Instrum.* **81**, 10D731 (2010).

<sup>4</sup>F. Scotti and R. E. Bell, *Rev. Sci. Instrum.* **81**, 10D732 (2010).

<sup>5</sup>D. B. Leviton, U.S. Patent No. 5,965,879 (12 October 1999).

<sup>6</sup>R. Majeski *et al.*, *Phys. Plasmas* **20**, 056103 (2013).